Electronic surface reconstruction and correlation in the fcc and dimer phases of RbC$_{60}$

Roberto Macovez,[1] Petra Rudolf,[1,2,*] Ingrid Marenne,[2] Lisbeth Kjeldgaard,[3] Paul A. Brühwiler,[3,4] Thomas Pichler,[5]
Paolo Vilmercati,[6] Rosanna Larciprete,[6] Luca Petaccia,[6] Giovanni Bertoni,[7] and Andrea Goldoni[6]

[1]*Zernike Institute for Advanced Materials, University of Groningen, Nijenborgh 4, NL-9747 AG Groningen, The Netherlands*
[2]*LISE, Facultes Universitaires Notre-Dame de la Paix, Rue de Bruxelles 61, B-5000 Namur, Belgium*
[3]*Department of Physics, Uppsala University, Box 530, S-75121 Uppsala, Sweden*
[4]*Empa, Swiss Federal Laboratories for Materials Testing and Research, Lerchenfeldstrasse 5, CH-9014 St. Gallen, Switzerland*
[5]*Institut für Festkörperforschung, IFW Dresden e.V., P.O. Box 270016, D-01171 Dresden, Germany*
[6]*Sincrotrone Trieste, Strada Statale 14 km 163.5, Area Science Park, I-34012 Trieste, Italy*
[7]*Laboratorio Nazionale TASC-INFM, Strada Statale 14 km 163.5, Area Science Park, I-34012 Trieste, Italy*

A combined photoemission and x-ray absorption study of a RbC$_{60}$ crystalline film is presented. We find evidence for an electronic charge reconstruction of the film surface in both the fcc and the dimer phases of RbC$_{60}$. We confirm the previous conclusion on less crystalline films that the dimer phase is insulating. Several observations, such as the presence of molecular features in the photoemission spectra, indicate that at least partial electron localization occurs in the high-temperature fcc phase. In the fcc phase, the surface consists in a half-charge C$_{60}$(111) plane and appears weakly metallic, as found for the bulk. In the dimer phase, the charge reconstruction simply implies the presence of neutral C$_{60}$ in the surface layer. The identification of neutral molecules in the surface layer drastically improves the agreement between calculations of the electronic density of states and photoelectron spectra in both phases.

PACS number(s): 79.60.Bm, 71.20.Tx, 71.27.+a

I. INTRODUCTION

Alkali-fulleride salts have been intensely studied over the past 15 years. In most cases, the charge transfer from the alkali metal to the fullerene is complete, so that the electronic structure of these compounds derives in a straightforward way from the molecular orbitals of the fullerene species involved. Despite this apparent simplicity, the wide range of different electronic properties displayed by these molecular solids is not fully understood. In particular, the interpretation of the experimental evidence provided by photoemission spectroscopy is still a subject of debate,[1–3] while also generating new insights.[4,5]

Alkali-intercalated fullerides are usually characterized by strong electron correlation. For cubic phases containing (C$_{60}$)$^{n-}$ ions, odd stoichiometries are either correlated metals or Mott insulators depending on the lattice spacing,[6–8] while even stoichiometries are driven insulating by Jahn-Teller coupling.[9,10] In noncubic monomer compounds, a weak crystal-field splitting of the t_{1u} states induces an insulating ground state. In phases where the fullerene molecules are bridged by intermolecular bonds, dimers are nonmagnetic and insulating,[11] while phases containing doubly bonded polymer chains display a temperature – or pressure-driven metal-to-insulator transition.[12,13]

Alkali fullerides with stoichiometry AC_{60} (A=K, Rb, and Cs), the last ones to be discovered,[14–17] are fascinating fullerene-derived salts displaying a variety of different electronic and structural phases. Above 400 K, the stable form of AC_{60} is a fcc lattice of rapidly spinning monomers.[18] At room temperature, a conducting phase of polymer chains sets in,[12,19,20] which is unstable towards a metal-to-insulator transition at lower temperature.[13] Two metastable phases are obtained by quenching from the fcc phase. Very fast cooling to

about 50 K results in an orientationally ordered simple cubic monomer phase[16] with rather unusual metallic properties.[21,22] Quenching to 200 K leads to the formation of singly bonded (C$_{60}$)$_2^{2-}$ dimers[11,17,23] that are isostructural and isoelectronic to the azafullerene molecule (C$_{59}$N)$_2$.[24] While NMR (Ref. 18) and electron spin resonance[13] investigations on the fcc phase revealed a high degree of localization of the unpaired electrons on individual C$_{60}$ molecules, optical conductivity measurements[25] found a metallic character, pointing to the correlated nature of the fcc phase. Like solid (C$_{59}$N)$_2$, the metastable dimer phase is insulating and diamagnetic, which derives from the fact that one electron *per cage* participates in the dimer bond and the nondegenerate orbital close to the Fermi level is totally filled.[24]

The valence-band photoemission features of fcc AC_{60} are much broader[26,27] than those of solid C$_{60}$.[28] The feature derived from the lowest unoccupied molecular orbital (LUMO), in particular, is found to be much wider than predicted by band-structure calculations for a partially filled t_{1u}-derived band (the full LUMO bandwidth is calculated to be 0.5 eV),[29] a situation encountered also in other alkali fullerides such as Rb$_3$C$_{60}$ and K$_3$C$_{60}$. As in A_3C$_{60}$ at high temperature,[1,30–32] the photoemission spectrum of the high-temperature phase of AC_{60} does not display a clear signature of a Fermi edge,[26,27] contrary to the expectation for a simple metal. For the dimer phase as well, the disagreement between the calculated occupied density of states (DOS) and the valence-band photoemission data is marked. While photoemission spectrum of solid (C$_{59}$N)$_2$ is identical to the theoretical DOS of the isolated azafullerene dimer,[24] a much worse agreement is found for dimerized RbC$_{60}$ (see Fig. 2 below).

Photoemission spectroscopy is particularly sensitive to the surface region, and modifications of the crystal and elec-

tronic structure are well known to occur at the surface of ionic compounds. As both pristine C_{60} and $(C_{59}N)_2$ are van der Waals solids while RbC_{60} is an ionic salt, it seems plausible that surface effects might be at least partially responsible for the discrepancy between calculation and experiment in RbC_{60}. The dimer and fcc phases of RbC_{60} are simple systems on which to test the importance of surface effects on the electronic structure of molecular solids.

Here, we present a combined valence-band and core-level photoemission spectroscopy (PES) and x-ray absorption spectroscopy (XAS) study of the fcc and dimer phases of a $RbC_{60}(111)$ thin film. We show that the film in the fcc and dimer phases is C_{60} terminated and the surface layer carries a lower net charge than the equivalent planes in the bulk. Finally, we discuss the electronic character of the surface of fcc RbC_{60} as compared to the bulk of the same phase.

II. EXPERIMENT

The experiments were performed in the ultrahigh vacuum chamber of the SuperESCA beamline[33] at the ELETTRA synchrotron radiation facility (base pressure $<5 \times 10^{-11}$ mbar). The Ag(100) substrate was mounted on a He-cooled manipulator and heated with a filament placed behind it. The temperature was monitored via a thermocouple inserted in a hole on the side of the sample. A phase pure $RbC_{60}(111)$ thin film was grown by intercalating a $C_{60}(111)$ film with an understoichiometric amount of Rb, followed by a vacuum distillation at 525 K to yield the fcc phase.[15] The dimer phase was then obtained by rapid cooling to 175 K at a rate of 50 K/min.

The photoemission spectra were acquired in two emission geometries to study the difference between the surface and bulk features of the film. In normal-emission (NE) geometry, photons impinge on the sample at 70° from the normal. In grazing emission (GE), the photon flux is normal to the surface and photoelectrons are analyzed at an angle of 70°. Due to the finite inelastic mean free path of electrons in a solid, the probed depth is lower in grazing than in normal emission. Each phase was measured at a temperature at which it is known to be stable: 175 K for the dimer phase, room temperature for the polymer, and 525 K for the fcc phase.

The binding energy was calibrated by recording the Fermi edge of the clean silver substrate. The Rb $3d$ and C $1s$ PES spectra were measured at a photon energy of 400 eV with a resolution of 0.15 eV, while for the valence-band (VB) spectra the photon energy was 129 eV and the resolution 0.036 eV. Photon energies were chosen in order to assure that the photoelectron kinetic energy and hence the electronic mean free path were roughly the same for VB and C $1s$ electrons, and large enough so that the photoemission spectra were not sensitive to modulations in the empty density of states.

All core-level spectra were fitted with curves obtained as convolutions of a Lorentzian and a Gaussian (Voigt functions) to mimic the molecular disorder and the experimental resolution. A Shirley background was added to account for secondary electrons. The Lorentzian width was fixed 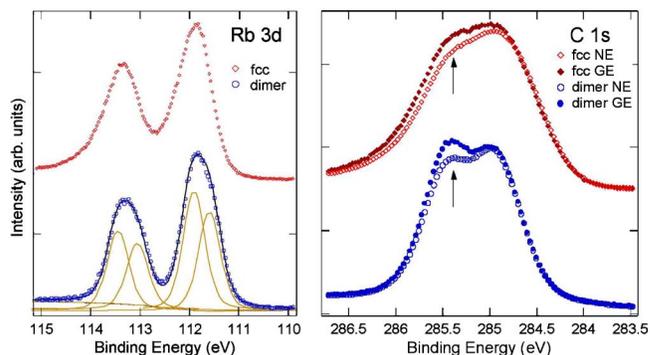to 80 meV to account for the core-hole lifetime (see, for example, Refs. [34] and [35]). While the spectra of the dimer phase were fitted with symmetric Voigt functions, in the fit of the fcc spectra a slight asymmetry toward high binding energy was introduced phenomenologically. This was accomplished by calculating the value of the convolution at each point distant d from the centroid on the high binding energy side with a variable Gaussian width scaled up by a factor $(\beta d+1)^{1/2}$, where β is a fit parameter which was found to be close to 0.5 for the fcc spectra. This procedure accounts for different sources of asymmetric and symmetric broadening (such as Franck-Condon broadening, inelastically scattered electrons, molecular disorder, and experimental resolution) and avoids using Doniach-Sunjic line shapes, which are suited for conventional metals but are probably not appropriate for correlated molecular systems.

The XAS spectra were acquired by measuring the carbon KVV Auger yield at 250 eV kinetic energy as the photon energy was varied across the C $1s$ absorption edge, and were corrected for beamline throughput by dividing by the current on a clean gold mesh. The photon energy calibration was obtained by comparing first- and second-order photoemission signals from suitable core levels.

III. RESULTS AND DISCUSSION

A. Core-level analysis: Surface termination and surface inequivalent C_{60} molecules

The core-level photoemission spectra of both RbC_{60} phases are shown in Fig. 1. The spectra of the dimer phase are sharper than those of the fcc phase due to the lower acquisition temperature, and the peaks appear more symmetric than in the fcc phase, which is related to the insulating character of the dimer phase. The Rb $3d$ normal-emission spectrum of the fcc phase consists of a single spin-orbit split doublet with the expected intensity ratio (2:3) and an energy separation of 1.5 eV. The presence of a single Rb component indicates that only octahedral sites are occupied, consistent with phase-pure fcc RbC_{60}.[15] In the dimer phase, the Rb $3d$ spectrum is structured, revealing the presence of two nonequivalent Rb contributions of similar intensity, as expected

FIG. 1. (Color online) Core-level photoemission spectra of fcc and dimer RbC_{60}. Left panel: Rb $3d$ region, collected at normal emission (for the dimer phase, the fit with two spin-orbit split components is also shown). Right panel: the corresponding C $1s$ photoemission spectra, collected at normal and 70° emission angle.

since the dimerization requires the existence of two non-equivalent Rb sites. The dimer phase spectrum could be reproduced (as also shown in Fig. 1) with two doublets of the same intensity ratio and energy splitting observed in the fcc phase. Negligible angle dependence is observed in both phases (not shown).

The RbC$_{60}$(111) film remained stable for several days in vacuum. The good stability of the surface implies that the film cannot be Rb terminated, since surface Rb would react with gaseous species. Moreover, the ratio of the Rb 3d and C 1s photoemission intensities is less than expected for the RbC$_{60}$ stoichiometry, indicating that the Rb signal is attenuated by the C$_{60}$ surface layer. Hence the distillation procedure yields a C$_{60}$-terminated RbC$_{60}$(111) film.

The C 1s spectra of the dimer and fcc phases are seen to contain (at least) two components, approximately 0.6 eV apart. The intensity of the two C 1s components varies with the emission angle. The one at higher binding energy (see arrows in Fig. 1, right panel) is more intense in grazing than in normal emission. Spectra from similar samples collected in normal emission and 80° grazing emission with a photon incidence angle of 40° in both cases showed the same changes in the C 1s intensities (not shown here). This implies that this intensity change cannot be due to a polarization dependence. Regarding the origin of the two components, we can exclude the fact that they arise from phase segregation into islands of RbC$_{60}$ and pure C$_{60}$, since the observed relative intensities of the two peaks are found to be the same regardless of the initial stoichiometry of the precursor film, and, moreover, pure C$_{60}$ sublimes at 455 K, i.e., below the distillation temperature.[15]

The C 1s binding energy of individual C atoms on a monomer or a dimer can, in principle, be slightly dependent on their position on the molecule due to different values of the Madelung potential closer or farther from surrounding ions or intermolecular bonds. However, as discussed in detail in Ref. 36, studies of chemisorbed C$_{60}$ suggest that intramolecular Madelung potential-like effects are quite small for C$_{60}$, presumably due to the excellent internal polarization of the molecule upon charging.[37] Therefore, we attribute the observation of distinct components in the C 1s spectrum to the existence of different molecular sites rather than to different atomic sites on the same molecule. In the following, we shall accordingly speak of distinct C$_{60}$ components when referring to the C 1s and valence-band spectra. The large width of each component (full width at half maximum ≈0.85 eV) reflects a combination of the aforementioned modulation in Madelung potential, the experimental resolution, and the effect of electron-phonon coupling.

From the relatively high interlayer separation ($d \approx 9$ Å) and the low electronic mean free path in C$_{60}$ compounds ($\lambda = 5 - 6$ Å, see Refs. 36 and 38) at the kinetic energies of the photoelectrons in the present experiment, the expected contribution of the surface C$_{60}$ layer to the normal-emission signal is $1 - \exp(-d/\lambda) \approx 75\% - 80\%$ of the total intensity. Hence only the first two or three C$_{60}$ layers give a detectable contribution to the photoemission signal, and the latter predominantly reflects the emission from the top C$_{60}$ surface layer. Therefore, the grazing emission spectra are practically sensitive to the topmost layer only due to an increase of the exponent by a factor of $1/\cos(70°)$. The fact that the two C 1s components are present in the GE spectra (with only small intensity changes compared to the NE spectra) clearly indicates that the two nonequivalent C$_{60}$ molecular sites are present at the film surface. Hence we rule out a surface core-level shift[37] as the origin of the two components in the PES spectra (i.e., bulk and surface components, although a small "bulk" contribution may be expected below the lower binding energy component in the NE spectra). Moreover, the double-peak feature is also observed in the polymer phase spectra (not shown here), implying that the occurrence of two nonequivalent molecular sites at the film surface has a common origin in all three phases.

B. Origin of two kinds of C$_{60}$ molecules at the surface

With the discussion above, we have demonstrated that the more likely interpretation of the two C 1s peaks is the presence of two kinds of C$_{60}$ molecules in the surface layer. Now we discuss the possible origin of these nonequivalent surface C$_{60}$ molecules.

The (111) surface of fcc RbC$_{60}$ is an example of a termination of an ionic compound with a maximum polarity plane. If the surface C$_{60}$ layer were fully charged, there would be an uncompensated negative charge at the film surface, and such termination would be electrostatically unstable.[39] In fact, polar terminations with uncompensated charges are never observed in nature. There are various ways in which the instability of a fully polar surface of an ionic solid is avoided, the most common being relaxation and buckling reconstruction. A surface relaxation can be excluded for RbC$_{60}$, as it does not introduce the nonequivalence between surface sites required to explain our C 1s core-level data. On the other hand, a buckling reconstruction would appear with a characteristic surface diffraction pattern, while the low-energy electron diffraction (LEED) of the film showed simply a (1×1) hexagonal pattern, in agreement with previous studies.[26] Also, the size and mass of the C$_{60}$ molecule suggest that a structural surface reconstruction might not be as energetically favorable as in conventional solids, where the ionic masses involved are much smaller.

A less common mechanism which can resolve the electrostatic instability of the RbC$_{60}$(111) surface, and at the same time explain the observation of two nonequivalent surface sites, is an electronic reconstruction in which the surface C$_{60}$ layer carries a lower net charge than the corresponding bulk layers.[40] This phenomenon has been observed on ultrathin films of ionic compounds,[41] at the interfaces between transition metal oxides,[42] and it was also recently proposed for fcc K$_3$C$_{60}$(111).[2,36,40]

To obtain a plausible value for the surface charge density, we follow Fripiat *et al.*[39] If one considers a thin slab or a semi-infinite crystal of a fcc ionic solid with (111) surface(s), the electrostatically stable termination must carry a surface charge density reduced to *half* its value inside the solid in order for the total dipole moment perpendicular to the surface to vanish. In the case of C$_{60}$-terminated RbC$_{60}$(111), the average charge in the surface layer is therefore 0.5e per molecule.

Half-integer ionic charges are, in fact, observed in other examples of surface and interface electronic reconstructions, in particular, in Na-terminated ultrathin NaCl films where the formal charge of the cations was reported to be $+0.5e$, implying a half-filled Na $3s$ band.[41] In RbC_{60} the difference in energy between the highest occupied molecular orbital (HOMO) and the LUMO is much less than that between the Na $2p$ and $3s$ states in NaCl, so that an electronic reconstruction is energetically more favorable.

Since in fcc RbC_{60} the electrons are mostly localized on single molecules,[13,18] a surface charge of $-0.5e$ per C_{60} actually corresponds to a situation in which half the molecules are neutral and half carry a $-1e$ charge, at least on a short time scale such as that of the photoemission process (shorter than 10 as). As the singly bonded dimer is stable only when it carries a net charge, in the transition to the metastable phase only the charged C_{60}^{1-} monomers take part in the dimerization, while the neutral monomers at the surface must remain so also at low temperature. The metallicity of the fcc phase implies that the localization of an electron on a specific molecule is limited to a finite time due to hopping processes. The observation of a (1×1) hexagonal LEED pattern suggests that no long-range charge ordering exists on the surface, or that on the longer LEED time scale, the nonequivalence between neutral and charged surface C_{60} monomers is averaged out.

Within the present model, therefore, the two components visible in the C $1s$ spectra reflect the presence of 50% neutral and 50% charged fullerene molecules in the surface layer. We assign the component at lower binding energy to the charged C_{60} species and the one at higher energy to neutral C_{60}, based on the relative intensity and angular dependence of the two C $1s$ components in both phases. This consideration is also true for the other molecular levels, for example, the HOMO (see below).

To support this assignment, we can roughly estimate the C $1s$ or HOMO photoemission binding energy difference (ΔBE) between the charged and neutral molecules, following the ideas of Ref. 36. We take as an ansatz a model in which the surface consists of alternate arrays of charged and neutral molecules. The binding energy difference ΔBE is approximately the difference in ionization potential between the two charge states (this is true even if the absolute energy of a given molecular orbital in the ground state of the system is not the same for charged and neutral molecules, see below). We start the calculation with the ionization of a neutral molecule by expelling an electron from the HOMO. The difference in ionization potential is evaluated as the cost of transferring the resulting hole to a distant negatively charged molecule. Such cost is, in general, the sum of an intramolecular Coulomb energy term plus an extramolecular Coulomb energy term (Madelung potential); the latter can be estimated in a simple way by considering the contribution of nearest neighbors (nn) only.[36] A charged surface molecule has two charged nn in the surface plane and three in the subsurface layer, for a total of 5, while a neutral molecule has four plus three, all other nn being neutral.

To move the hole in the HOMO of a C_{60}^{1+} molecule to the HOMO of a distant C_{60} ion, we have to consider that there is an initial configuration Madelung contribution from the C_{60}^{1+}

of $-7V$ and from the C_{60}^{1-} of $+5V$, for a total of $-2V$, where V is the screened Coulomb potential energy between singly charged nn ions. In the final state configuration, both molecules are neutral, giving no terms in V, but the formerly negatively charged molecule now contains an exciton. The change in internal energy between the initial and final configurations of such a molecule is simply the exciton binding energy or E_{ex}. If there is a misalignment in the ground state of the system between the HOMO levels of the neutral and charged molecules due to solid-state effects, we postulate that to a large extent such band (mis)alignment is maintained in the final state of the PES process, as this occurs on rather fast time scales. Hence the binding energy difference is simply the ionization potential difference or $\Delta BE = 2V - E_{ex}$, placing the spectrum from the negatively charged molecules at higher energy (or lower BE). Using the values found for solid C_{60}, namely, $E_{ex} = 1.5$ eV for surface excitons[43] and $V = 0.3$ eV,[44] we find a binding energy difference of 0.9 eV, in reasonable agreement with our experimental data. As the exciton binding energy is roughly the same for both core and valence excitons,[45] our estimate is valid for the C $1s$ level as well as for higher-lying molecular orbitals. The fact that we have slightly overestimated the experimental binding energy separation is possibly related to the fact that the screening of Coulomb interactions could be more efficient in a weakly metallic environment as that of RbC_{60} than in van der Waals fullerite. This seems to be suggested also by other theoretical[46] and experimental[47] studies.

In our mathematical reconstruction of the core-level and valence-band spectra (see Section III C) at NE (Fig. 2), we find that in the fcc phase, the spectral weight of the C_{60}^{1-} component is about 62%, implying that at normal emission a fraction of the signal equal to $\sim$25% of the total spectral weight comes from the subsurface (bulklike) layers where all the molecules are C_{60}^{1-}, in agreement with the low inelastic mean free path.[36,38] A fit of the normal-emission C $1s$ spectra of the dimer phase allowing for different component widths gives a slightly lower bulk-to-total-signal ratio (15%), possibly related to the different surface morphology of the dimer phase.[48]

C. Valence-band analysis

Similarly to core-level spectra, the VB electronic structure of RbC_{60} reflects the contribution of both charged and neutral species. The photoemission features in the VB spectra of both RbC_{60} phases (Fig. 2, right panel) originate entirely from fullerene orbitals, since the highest occupied Rb core level lies around 18 eV binding energy. Their positions and shapes are in agreement with previous photoemission studies.[26,49] The features in fcc RbC_{60} are much broader than those of pristine C_{60}. There is an evident discrepancy also between the theoretical DOS of the $(C_{60})_2^{2-}$ dimer[24] and the photoemission spectrum of dimerized RbC_{60}, except for the states at lowest binding energy, which arise from the highest occupied molecular orbitals of the charged dimer. We note that such states are not derived from the orbitals of the isolated C_{60} monomer, but are wholly different states, characteristic of the dimer molecule, which has a different chemical
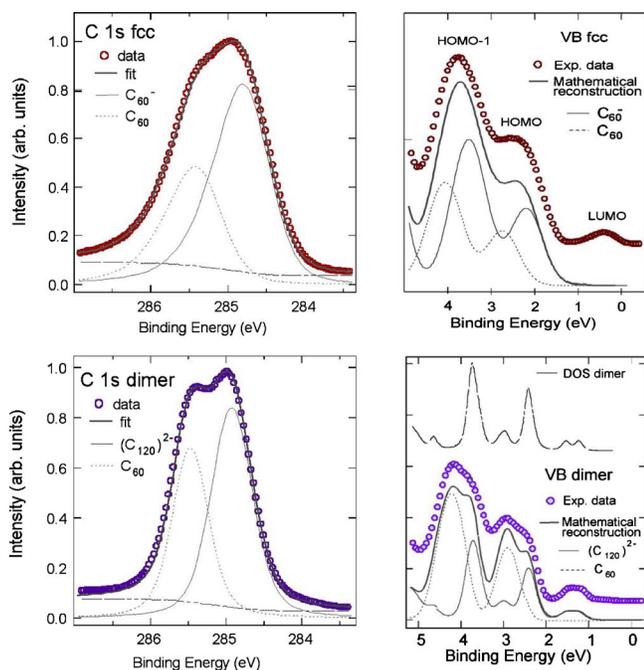
FIG. 2. (Color online) Left: C $1s$ photoemission spectrum of the fcc phase of RbC$_{60}$, taken in normal emission (NE), fitted with two components of the same width (upper panel, see Sec. II for details). Analogous fit of the C $1s$ NE spectrum of the dimer phase assuming that the charged component has a larger width due to the molecular distortion (lower panel). Right: comparison between the valence-band photoemission spectra of fcc RbC$_{60}$ and the valence band of fcc C$_{60}$, taken in NE geometry at $h\nu = 133$ eV (upper panel). The peaks at 3 and 4 eV binding energy in the spectrum of pristine C$_{60}$ are the bands derived from the C$_{60}$ HOMO and HOMO-1 levels, respectively. In the lower panel, the valence-band spectrum of the dimer phase of RbC$_{60}$ is compared to the calculated DOS for the $(C_{60})_2^{2-}$ dimer (Ref. 24). The spectral intensity between 1 and 1.8 eV binding energy derives from the highest occupied molecular states of the charged $(C_{60})_2^{2-}$ dimer. The result of a mathematical reconstruction of both VB spectra with two components are also shown (see text). The feature closest to the Fermi level in the spectrum of fcc RbC$_{60}$, which derives from the partial filling of the C$_{60}$-derived LUMO, is not reproduced.

formula, structure, and symmetry than the monomer.

By aligning the calculated and measured spectra so that the highest occupied molecular orbitals of the charged dimer overlap, as shown in Fig. 2, the other peaks in the theoretical DOS are superimposed to experimental features which appear as shoulders of the most prominent peaks in the spectra. These observations have a straightforward interpretation in view of our analysis, as neutral C$_{60}$ monomers coexist at the film surface with either $(C_{60})_2^{2-}$ dimers or charged C$_{60}$ monomers. The spectrum of dimerized RbC$_{60}$ was reproduced as the sum of a C$_{60}$ VB line shape (using data acquired in the same experimental conditions before Rb doping and distillation) and the theoretical $(C_{60})_2^{2-}$ DOS,[24] broadened to mimic the experimental resolution and inelastic electron scattering, and shifted and adjusted in intensity to best reproduce the various spectral features. The energy separation between the two components is similar to that found in the C $1s$ spectra of the dimer phase (see Sec. III A).
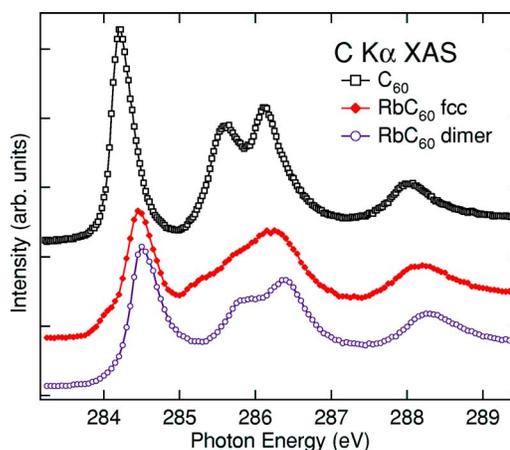

FIG. 3. (Color online) C $1s$ x-ray absorption spectra for the dimer and fcc phases of RbC$_{60}$ compared to that of pristine C$_{60}$. The spectra are normalized to the area under the curve between 285 and 287 eV photon energy (see text).

The RbC$_{60}$ fcc valence-band spectrum was reconstructed using two C$_{60}$ line shapes, corresponding to the neutral and charged monomers, with approximately the same relative intensity and energy separation observed in the core-level spectra, as expected from our previous discussion of the binding energy difference between the two charge states. The energy separation between the HOMO of the negatively charged component and the LUMO-derived feature, which represents the band gap of the charged molecules in this phase, is found to be 1.7–1.8 eV (centroid to centroid). This value is intermediate between the gap found for the neutral molecules in pristine fullerite and that observed in A_6C$_{60}$ compounds.[50] This could be anticipated, as the lower filling of the LUMO entails a reduced relaxation of the molecular orbitals, and provides further support to our interpretation.

Good overall agreement is reached by the two-component model of the valence-band spectra for both phases, though the quality is not quite as good as that for the core-level fits. We believe that the asymmetry and Shirley tailing of each component due to inelastically scattered electrons, as well as broadening due to the wider range of Madelung potentials present at the film surface, should be included for a more accurate reconstruction of the valence spectra.

D. XAS spectra

Our interpretation of the photoemission spectra in terms of different charge states of the surface molecules is further supported by XAS. The XAS spectra of both the dimer and fcc phases of RbC$_{60}$ appear more structured than the corresponding spectrum of pristine C$_{60}$, as shown in Fig. 3. The features in the fcc RbC$_{60}$ spectrum are broader than in pristine C$_{60}$, which is presumably largely due to the elevated temperature.

The XAS spectra are normalized to the area under the features between 285 and 287 eV photon energy, which in the C$_{60}$ monomer correspond to C $1s \rightarrow$ LUMO+1 and C $1s \rightarrow$ LUMO+2 transitions. With this normalization, also the line shapes at high photon energies overlap. The height of

the first absorption resonance, corresponding to the C 1s →LUMO transition, is reduced in both dimer and fcc phases of RbC$_{60}$ by almost one-half with respect to pristine C$_{60}$. This can be accounted for if the most prominent absorption feature in the dimer and fcc spectra arises from the neutral surface monomers, which correspond to 50% of the surface layer. The total intensity (area under the curve) between the onset and 285 eV in the RbC$_{60}$ spectra is reduced by 15% compared to the total intensity of the C 1s→LUMO transition in pristine C$_{60}$. This result, given the uncertainty involved, is consistent with an average partial filling of the LUMO in our RbC$_{60}$ film of close to or less than 1/6, as expected for AC$_{60}$ stoichiometries.

The C 1s binding energy measured with PES (roughly 285 eV for the charged component at lower BE, see Fig. 2) is higher than the XAS onset in both RbC$_{60}$ phases, which implies that metallic screening as it is found in conventional metals, or in some C$_{60}$ monolayer systems, is not present here, which points to a predominantly molecular character of both phases similar to what is observed in pristine fullerite[43,51] and K$_3$C$_{60}$ (Ref. 52; see also Ref. 53 and Sec. V B of Ref. 35 for a discussion).

In the spectrum of fcc RbC$_{60}$, the onset of absorption occurs at lower photon energy than in the dimer phase spectrum, and the peaks in the latter appear to be shifted to slightly higher photon energies. Examining the spectrum of fcc RbC$_{60}$ in more detail, we note that the main absorption peak at 284.5 eV is accompanied by a shoulder at lower photon energy, and a similar shoulder is visible slightly above 285 eV photon energy preceding the higher π^*-derived features between 285.5 and 286.5 eV. Since both features disappear in the dimer XAS spectrum, it is reasonable that they have a common origin. As the binding energy of the charged molecules is lower, we associate the onset of absorption with processes involving charged molecules rather than neutral ones.

There are two possible excited XAS states for a charged molecule since the spin of the LUMO electron in the ground state may be parallel or unparallel to the spin of the core hole (i.e., the spin of the excited electron). The prepeak around 284 eV photon energy probably originates then from the parallel-spin excited state in the charged monomers, assuming that the most important contribution to the exchange energy comes from Hund's rule coupling between the two electrons sitting in the LUMO states.

The relative intensity between the shoulder at 284 eV and the main C 1s→LUMO absorption peak at 284.5 eV of photon energy can be rationalized assuming that the unparallel-spin C 1s→LUMO excitations in the charged molecules and the C 1s→LUMO excitations in the neutral C$_{60}$ molecules both contribute to the main absorption peak, and considering that for parallel-spin C 1s→LUMO excitations, the absorption process is only allowed for a target orbital different (orthogonal) from the LUMO already occupied in the C$_{60}^{1-}$ ground state. Since the XAS were measured in partial yield collecting electrons at 250 eV kinetic energy this means that 70% of the signal comes from the surface (35% C$_{60}$ and 35% C$_{60}^{1-}$) and 30% from the layers underneath (all C$_{60}^{1-}$). So, 65% of the signal should come from C$_{60}^{1-}$. Of this 65%, 3/5 correspond to unparallel-spin excitations and 2/5 to parallel-

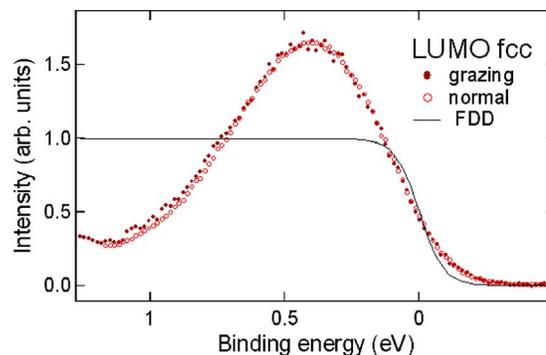FIG. 4. (Color online) Photoemission spectra of the C$_{60}$ LUMO-derived states in fcc RbC$_{60}$ for both emission geometries, compared to the Fermi-Dirac distribution (FDD) at 525 K. The spectra are normalized so that the spectral intensity is 0.5 at the Fermi energy.

spin excitation. According to our interpretation, we have that (2/5)(65%)=26% is the weight roughly expected for the onset peak (parallel-spin LUMO electrons). Now the strongest assumption is that the excitation with unparallel-spin LUMO electrons contributes to the main peak (roughly at the same absorption energy of the neutral C$_{60}$ molecules). In this way, we have 26% weight to the onset shoulder and (3/5) ×(65%)+35%=74% weight on the main peak, in agreement with the experimental spectrum.

The XAS spectra of the two RbC$_{60}$ phases studied here look very similar, despite the fact that the unoccupied states of the C$_{60}^{1-}$ monomer and those of the (C$_{60}$)$_2^{2-}$ dimer are very different. This similarity, together with the fact that the XAS spectrum of fcc RbC$_{60}$ does not seem to consist simply of two components of comparable intensity, is a strong hint that an important contribution to the absorption spectrum of both RbC$_{60}$ phases comes from the neutral C$_{60}$ molecules present at the film surface.

E. Surface and bulk metallicity in the fcc phase

Finally, we discuss the metallic character of the fcc phase. We compare the grazing and normal emission PES spectra of the C$_{60}$ LUMO-derived feature in the fcc phase of RbC$_{60}$ in Fig. 4. The LUMO-derived spectrum looks practically identical in the two geometries, with a single broad feature centered at 0.5 eV binding energy and a very low but nonzero spectral density at the Fermi level as previously observed in both fcc RbC$_{60}$ and CsC$_{60}$.[26,27,49] Although the signal in the grazing emission spectrum comes almost completely from the surface layer (while in normal emission about 25% of the signal comes from the layer underneath) and only 50% of the surface molecules are charged, no angular dependence is visible in the LUMO-derived signal, contrary to the observations on the other molecular levels. The fact that the binding energy of the LUMO-derived feature is the same in both geometries and that it crosses the Fermi level suggests that both the surface and the bulk of fcc RbC$_{60}$ are (weakly) metallic, which results in the alignment of the chemical potentials of bulk and surface.

Within the same model used to account for the binding energy differences, we can discuss the metallic character of

the surface and the bulk of RbC_{60}. A long-distance hopping process in the bulk of RbC_{60} between two singly charged molecules costs an energy amount equal to the (rather large) Hubbard U in this phase. Despite this, the kinetic energy gain derived from hopping is apparently large enough to keep RbC_{60} as well as other alkali fullerides of odd stoichiometry on the metallic side of a Mott-Hubbard transition.[54] At the film surface, a long-distance hop from a charged molecule to a neutral one leads to a net intermolecular repulsive energy loss of $2V < U$. In other words, although there is no on-site U to pay for the hopping process to occur, the nearest-neighbor Coulomb repulsion tends to inhibit conduction in the surface layer. Although in the surface layer the bandwidth should be reduced, this could be compensated by the decrease in the energy barrier for the hopping process compared to the bulk. This explanation would rationalize the apparent similarity in the electronic character of bulk and surface, despite the occurrence of the surface charge reconstruction. We cannot rule out, however, the possibility that the surface layer is actually a small gap insulating system.

The width of the LUMO feature is much larger than ~ 0.1 eV predicted by band theory for the singly occupied t_{1u} band,[29] because it is dominated by electron-electron and, especially, electron-phonon interactions. While both the electron-electron and electron-phonon couplings, in general, lead to a narrowing of the electronic bandwidth, they can give rise to satellites, which can result in an effective broadening of the PES feature. This is a well-known phenomenon already observed and discussed in other fullerides. In particular, Franck-Condon broadening has been extensively observed in C_{60}, for example, in PES experiments on C_{60} and C_{60}^{1-} in the gas phase,[55] on C_{60} films on graphite,[56,57] and on K_3C_{60} and Rb_3C_{60} films.[1,31,32] In the present case, the fact that electron-phonon broadening is a dominant effect in the photoemission spectra of RbC_{60} is indicated by the broadness of the spectral features of the dimer phase, where no band or correlation effects are present.

Another interesting feature in Fig. 4 is the small but finite intensity at and above the Fermi level. The spectral weight extends well above E_F and decays very slowly compared to the Fermi-Dirac distribution at the measuring temperature of 525 K. This is also observed in the photoemission spectra of A_3C_{60} fullerides at high temperature.[1,32] The observation of a similar phenomenon in both RbC_{60} and A_3C_{60} compounds suggests that it is not due to details of the bandlike electronic DOS. The decay of photoemission intensity at E_F with increasing temperature observed[1,32] in A_3C_{60} might reflect the transfer of spectral intensity from the coherent part of the one-electron removal spectral function to phonon-loss and phonon-gain satellites. The intensity of such satellites should, indeed, become the more important the higher the temperature, and be modulated by the electron-phonon coupling, which for LUMO (t_{1u}) electrons is strongest to the high-frequency intramolecular H_g modes.[58]

On the other hand, correlation effects are expected to be important in fcc RbC_{60}, where the LUMO electrons are mainly localized on single molecules.[13,18] The tailing of the spectral intensity above E_F in both AC_{60} and A_3C_{60} compounds at high T could be due either to Franck-Condon broadening or to the presence of a (polaronic) quasiparticle peak centered above E_F. Calculations[59] of the spectral function for the threefold degenerate Mott-Hubbard model in the localized limit with $U = 0.7$ eV show, in fact, that at low doping the spectral function has a pole near E_F, whose energy position depends on the number of electrons per site; namely, it is below the Fermi energy for $x = 1$, at E_F for $x = 0.8$, and slightly above E_F for lower doping levels such as that observed at the film surface ($x = 0.5$). (Also for $x \approx 1.5$ the spectral function has a pole right above E_F.) The complete lack of structure in the spectrum suggests that the spectral function at high temperature hardly contains any intensity from coherent features, which does not allow us to unambiguously ascribe the tail above E_F to electron-phonon or electron-electron coupling effects.

IV. CONCLUSIONS

Our combined photoemission and x-ray absorption study of the RbC_{60} fcc and dimer phases provides evidence for an electronic charge reconstruction of the film surface. These results confirm that surfaces and interfaces of C_{60} compounds can easily accommodate polar instabilities without giving rise to structural roughness, an observation which is relevant for the application of C_{60}-derived materials in organic-based junctions for electronic devices. We also found that the molecular character of the compound results in the electron charges being localized on single molecules on the photoemission time scale. For the dimer phase, the proposed electronic charge reconstruction brings calculations for the electronic density of states and the photoemission data in very good agreement. In the fcc phase, the film termination is a half-charge $C_{60}(111)$ plane, which might have a correlated character similar to the bulk of the same phase.

---

*Corresponding author. Electronic address: p.rudolf@rug.nl

[1] A. Goldoni, L. Sangaletti, S. L. Friedmann, Z.-X. Shen, M. Peloi, F. Parmigiani, G. Comelli, and G. Paolucci, J. Chem. Phys. **113**,

8266 (2000).

[2] J. Schiessling, L. Kjeldgaard, T. Käämbre, I. Marenne, L. Qian, J. N. O'Shea, J. Schnadt, M. G. Garnier, D. Nordlund, M. Nagas-

ono, C. J. Glover, J.-E. Rubensson, N. Mårtensson, P. Rudolf, J. Nordgren, and P. A. Brühwiler, Eur. Phys. J. B **41**, 435 (2004).

[3] R. Hesper, L. H. Tjeng, A. Heeres, and G. A. Sawatzky, Phys. Rev. B **62**, 16046 (2000).

[4] A. Goldoni, L. Petaccia, G. Zampieri, S. Lizzit, C. Cepek, E. Gayone, J. Wells, and Ph. Hofmann, Phys. Rev. B **74**, 045414 (2006).

[5] A. Tamai, A. P. Seitsonen, T. Greber, and J. Osterwalder, Phys. Rev. B **74**, 085407 (2006).

[6] J. E. Han, E. Koch, and O. Gunnarsson, Phys. Rev. Lett. **84**, 1276 (2000).

[7] P. Durand, G. R. Darling, Y. Dubitsky, A. Zaopo, and M. J. Rosseinsky, Nat. Mater. **2**, 605 (2003).

[8] P. A. Brühwiler, A. J. Maxwell, A. Nilsson, N. Mårtensson, and O. Gunnarsson, Phys. Rev. B **48**, 18296 (1993).

[9] V. Brouet, H. Alloul, L. Thien-Nga, S. Garaj, and L. Forro, Phys. Rev. Lett. **86**, 4680 (2001).

[10] M. Fabrizio and E. Tosatti, Phys. Rev. B **55**, 13465 (1997).

[11] G. Oszlányi, G. Bortel, G. Faigel, M. Tegze, L. Gránásy, S. Peckker, P. W. Stephens, G. Bendele, R. Dinnebier, G. Mihály, A. Jánossy, O. Chauvet, and L. Forró, Phys. Rev. B **51**, 12228 (1995).

[12] K. Khazeni, V. H. Crespi, J. Hone, A. Zettl, and M. L. Cohen, Phys. Rev. B **56**, 6627 (1997).

[13] O. Chauvet, G. Oszlányi, L. Forró, P. W. Stephens, M. Tegze, G. Faigel, and A. Jánossy, Phys. Rev. Lett. **72**, 2721 (1994).

[14] J. Winter and H. Kuzmany, Solid State Commun. **84**, 935 (1992).

[15] D. M. Poirier, Appl. Phys. Lett. **64**, 1356 (1994).

[16] M. Kosaka, K. Tanigaki, T. Tanaka, T. Atake, A. Lappas, and K. Prassides, Phys. Rev. B **51**, 12018 (1995).

[17] Q. Zhu, D. Cox, and J. E. Fischer, Phys. Rev. B **51**, 3966 (1995).

[18] R. Tycko, G. Dabbagh, D. W. Murphy, Q. Zhu, and J. E. Fischer, Phys. Rev. B **48**, 9097 (1993).

[19] P. W. Stephens, G. Bortel, G. Faigel, M. Tegze, A. Jánossy, S. Peckker, G. Oszlányi, and L. Forró, Nature (London) **370**, 636 (1994).

[20] S. Pekker, L. Forró, G. Mihály, and A. Jánossy, Solid State Commun. **90**, 349 (1994).

[21] V. Brouet, H. Alloul, F. Quéré, G. Baumgartner, and L. Forró, Phys. Rev. Lett. **82**, 2131 (1999).

[22] V. Brouet, H. Alloul, and L. Forró, Phys. Rev. B **66**, 155123 (2002).

[23] K.-F. Their, M. Mehring, and F. Rachdi, Phys. Rev. B **55**, 124 (1997).

[24] T. Pichler, M. Knupfer, M. S. Golden, S. Haffner, R. Friedlein, J. Fink, W. Andreoni, A. Curioni, M. Keshavarez, K. C. Bellavia-Lund, A. Sastre, J. C. Hummelen, and F. Wudl, Phys. Rev. Lett. **78**, 4249 (1997).

[25] M. C. Martin, D. Koller, X. Du, P. W. Stephens, and L. Mihaly, Phys. Rev. B **49**, 10818 (1994).

[26] G. P. Lopinski, M. G. Mitch, J. R. Fox, and J. S. Lannin, Phys. Rev. B **50**, 16098 (1994).

[27] M. De Seta, L. Petaccia, and F. Evangelisti, J. Phys.: Condens. Matter **8**, 7221 (1996).

[28] M. R. C. Hunt, P. Rudolf, and S. Modesti, Phys. Rev. B **55**, 7889 (1997).

[29] S. C. Erwin and W. E. Pickett, Science **254**, 842 (1991).

[30] M. S. Golden, M. Knupfer, J. Fink, J. F. Armbruster, T. R. Cummins, H. A. Romberg, M. Roth, M. Sing, M. Schmidt, and E. Sohmen, J. Phys.: Condens. Matter **7**, 8219 (1995).

[31] A. Goldoni, S. L. Friedmann, Z.-X. Shen, and F. Parmigiani, Phys. Rev. B **58**, 11023 (1998); A. Goldoni, L. Sangaletti, M. Peloi, F. Parmigiani, G. Comelli, and G. Paolucci, Surf. Sci. **482-485**, 476 (2001).

[32] M. Knupfer, M. Merkel, M. S. Golden, J. Fink, O. Gunnarsson, and V. P. Antropov, Phys. Rev. B **47**, 13944 (1993).

[33] A. Abrami, M. Barnaba, L. Battistello, A. Bianco, B. Brena, G. Cautero, Q. H. Chen, D. Cocco, G. Comelli, S. Contrino, F. DeBona, S. Di Fonzo, C. Fava, P. Finetti, P. Furlan, A. Galimberti, A. Gambitta, D. Giuressi, R. Godnig, W. Jark, S. Lizzit, F. Mazzolini, P. Melpignano, L. Olivi, G. Paolucci, R. Pugliese, S. N. Qian, R. Rosei, G. Sandrin, A. Savoia, R. Sergo, G. Sostero, R. Tommasini, M. Tudor, D. Vivoda, F.-Q. Wei, and F. Zanini, Rev. Sci. Instrum. **66**, 1618 (1995).

[34] M. Coville and T. D. Thomas, Phys. Rev. A **43**, 6053 (1991).

[35] P. A. Brühwiler, O. Karis, and N. Mårtensson, Rev. Mod. Phys. **74**, 703 (2002).

[36] J. Schiessling, L. Kjeldgaard, T. Käämbre, I. Marenne, J. N. O'Shea, J. Schnadt, C. Glover, M. Nagasono, D. Nordlund, M. G. Garnier, L. Qian, J.-E. Rubensson, P. Rudolf, N. Mårtensson, J. Nordgren, and P. A. Brühwiler, Phys. Rev. B **71**, 165420 (2005).

[37] E. Rotenberg, C. Enkvist, P. A. Brühwiler, A. J. Maxwell, and N. Mårtensson, Phys. Rev. B **54**, R5279 (1996); E. L. Shirley, L. X. Benedict, and S. G. Louie, *ibid.* **54**, 10970 (1996).

[38] A. Goldoni, L. Sangaletti, F. Parmigiani, G. Comelli, and G. Paolucci, Phys. Rev. Lett. **87**, 076401 (2001).

[39] J. G. Fripiat, A. A. Lucas, J. M. Andre, and E. G. Derouane, Chem. Phys. **21**, 101 (1977).

[40] R. Hesper, L. H. Tjeng, A. Heeres, and G. A. Sawatzky, Phys. Rev. B **62**, 16046 (2000).

[41] W. Hebenstreit, M. Schmid, J. Redinger, R. Podloucky, and P. Varga, Phys. Rev. Lett. **85**, 5376 (2000).

[42] N. Nakagawa, H. Y. Hwang, and D. A. Muller, Nat. Mater. **5**, 204 (2006).

[43] A. Goldoni, C. Cepek, and S. Modesti, Phys. Rev. B **54**, 2890 (1996); Synth. Met. **77**, 189 (1996).

[44] V. P. Antropov, O. Gunnarsson, and O. Jepsen, Phys. Rev. B **46**, 13647 (1992).

[45] J. Schnadt, J. Schiessling, and P. A. Brühwiler, Chem. Phys. **312**, 39 (2005).

[46] E. Koch, O. Gunnarsson, and R. M. Martin, Phys. Rev. Lett. **83**, 620 (1999); P. E. Lammert, D. S. Rokhsar, S. Chakravarty, S. Kivelson, and M. I. Salkola, *ibid.* **74**, 996 (1995).

[47] R. Macovez, M. R. C. Hunt, I. Marenne, A. Goldoni, M. Pedio, and P. Rudolf (unpublished).

[48] We assumed that in the dimer phase the charged component is broader than the neutral one because of the molecular distortion induced by the formation of the dimer bond.

[49] D. M. Poirier, C. G. Olson, and J. H. Weaver, Phys. Rev. B **52**, 11662 (1995).

[50] P. Rudolf, M. S. Golden, and P. A. Brühwiler, J. Electron Spectrosc. Relat. Phenom. **100**, 409 (1999).

[51] S. Krummacher, M. Biermann, M. Neeb, A. Liebsch, and W. Eberhardt, Phys. Rev. B **48**, 8424 (1993).

[52] T. Käämbre, J. Schiessling, L. Kjeldgaard, L. Qian, I. Marenne, J. N. O'Shea, J. Schnadt, D. Nordlund, C. J. Glover, J.-E. Rubensson, P. Rudolf, N. Mårtensson, J. Nordgren, and P. A. Brühwiler, Phys. Rev. B (to be published).

[53] A. J. Maxwell, P. A. Brühwiler, A. Nilsson, N. Martensson, and P.

Rudolf, Phys. Rev. B **49**, 10717 (1994).

[54] E. Koch, O. Gunnarsson, and R. M. Martin, Phys. Rev. B **60**, 15714 (1999).

[55] O. Gunnarsson, H. Handschuh, P. S. Bechthold, B. Kessler, G. Ganteför, and W. Eberhardt, Phys. Rev. Lett. **74**, 1875 (1995).

[56] P. A. Brühwiler, A. J. Maxwell, P. Baltzer, S. Andersson, D. Arvanitis, L. Karlsson, and N. Mårtensson, Chem. Phys. Lett. **279**, 85 (1997).

[57] N. Manini, P. Gattari, and E. Tosatti, Phys. Rev. Lett. **91**, 196402 (2003).

[58] C. M. Varma, J. Zaanen, and K. Raghavachari, Science **254**, 989 (1991).

[59] M. Meinders, Ph.D. thesis, University of Groningen, 1994.